www.rericjournal.ait.ac.th

Characteristics of Biogas-Hydrogen Engines in a Hybrid Renewable Energy System

Van Ga Bui*,[1], Trung Hung Vo[+], Thi Minh Tu Bui*, Le Bich Tram Truong*, and Thanh Xuan Nguyen Thi*

ARTICLE INFO

Article history:
Received 12 September 2021
Received in revised form
18 October 2021
Accepted 21 October 2021

Keywords:
Biogas
Hybrid renewable energy system
Hydrogen storage system
Renewable energy
Solar energy

ABSTRACT

Solar-biogas hybrid renewable energy system (HRES) is an effective way for electrification of rural area in the developing countries. When the power of the PV panels of the HRES is higher than that of the load, the excess energy is used to produce hydrogen through the water electrolyser. Hydrogen is then blended with biogas to fuel the internal combustion engine of the generator. A microcontroller connects the PV panels, the water electrolyser, and the consumed network to automatically start the generator when an additional power is needed. The addition of 20% hydrogen into biogas M7C3 leads to an increase in engine cycle work by 13%, 4% and 2% at 100%, 65% and 50% load operating mode, respectively. As compared to full load mode, CO and HC emissions of the engine are doubled, but the NO_x emission drops down 50% in the half load operating mode. Independently loading regime, the addition of hydrogen to biogas results in a decrease in CO and HC emissions, but an increase in NO_x emissions. At a given speed and engine loading mode, the optimal equivalence ratio and advance ignition angle decrease as increasing CH_4 composition in biogas or/and H_2 content in fuel blend.

1. INTRODUCTION

According to the International Energy Agency (IEA), the number of global population without access to electricity declined from 1,132 million in 2015 to 752 million in 2020. However, due to the COVID-19 pandemic, under worldwide current planned policies, an estimated 660 million people would still lack access in 2030 [2]. Most of these populations live in rural areas of developing countries [3]. To meet their minimum energy needs, people in these regions often use fossil fuels to operate generators [4]-[5]. This fact requires researchers to develop alternative power generation systems to meet the needs of the people while waiting for countries to have enough economic capacity to extend their electricity supply networks.

Rising energy demand and concerns related to pollution and GHG emissions due to the use of fossil fuels have led countries to turn to clean or renewable energy when setting up new power plants or extending their existing electricity networks [6]. Today, many countries and regions have made priority policies and taken effective measures to increase installed capacity of renewable energy systems [7]-[11]. The percentages of different types of renewable energy sources (RES) in the world are shown in Figure 1a. Hydroelectricity accounts for the highest proportion of RES, followed by wind and solar power. More than 80% of RES plants in the world are off grid (Figure 1b) [7].

Renewable energy sources can substitute fossil fuels in the future due to their abundance, diverse and clean characteristics [12]. Worldwide electricity production from RES increases steadily every year [13]. However, unlike fossil energy, the main disadvantage of renewable energy in most cases is its direct dependence on unpredictable and uncontrollable weather and environmental conditions, thus, it is difficult to ensure the reliability of the RES system [14]-[15].

It is clear that a single renewable energy source is not sufficient to support an uninterruptible energy supply system [16]. The use of a single power source often results in an over sizing system to compensate the energy requirement due to the randomness and discontinuity of the RESs [17]. This increases the capital cost of the system [7]. Besides, the imbalance between production and demand capacity will cause shortage or excess of power of the system [18]. When the electrical capacity produced by the system is less than the demand, additional power is required. Conversely, when the electrical capacity of the system exceeds the used capacity, it is necessary to store excess energy. Thereby, the load management system and the energy storage devices must be integrated into the RES systems [18]. Batteries are often used for energy storage [19]. They are activated when the RES capacity is not enough to meet the load demand. The cost of batteries accounts for an important proportion in the RES plants due to their

*University of Science and Technology – The University of Danang, Vietnam.

[+] University of Technology and Education – The University of Danang, Vietnam.

[1]Corresponding author:
Tel: +84 913 402 278.
Email: buivanga@ac.udn.vn

short life cycle that need to be replaced frequently during system operation [15]. This increases the energy cost of the RES plant in general.

Therefore, hybrid renewable energy systems (HRES) have been suggested to address the unavoidable and challenging obstacles of the RES [50], [13]. HRES can include numerous types of energy sources and, generally include at least two renewable or non-renewable sources [20]. Connecting different intermittent energy sources to dispatchable sources such as biogas, batteries or to a grid system provides a unique problem solution to the limitations of RES. HRES can reduce power generation fluctuations, helping to reduce the need for energy storage [16].

The energy cost of a hybrid renewable energy system is about 30% cheaper than that of fossil fuel-powered plant [21]. On the other hand, the components of the HRES can be optimized, thereby reducing costs of investment and operation [22]-[23]. Many RESs can be integrated into the HRES [50]. HRESs can operate in grid-connected and off-grid modes sustainably, lowering electricity costs and improve system reliability [15]. Many researchers have proved that the HRES is the most suitable electricity production, particularly for remote areas [24].

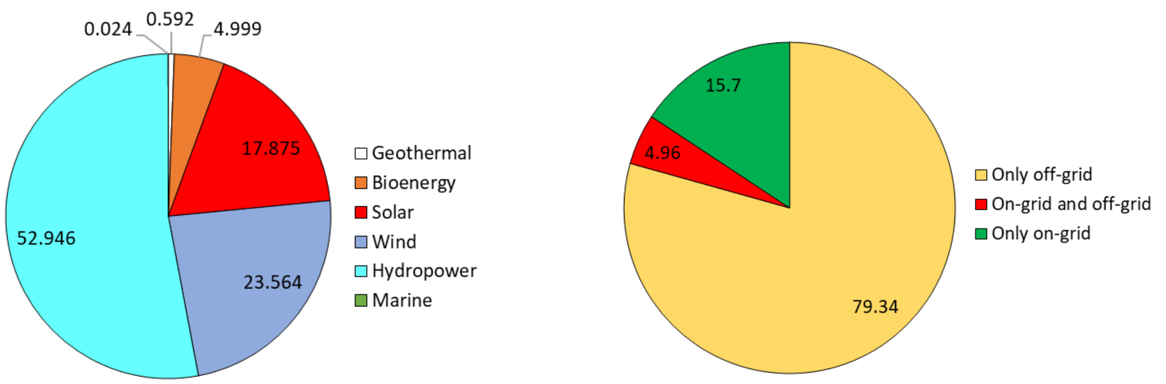

(a) (b)

Fig. 1. Percentage of installed capacity of different RES (a), and characteristic of RES (b) in the world 2017 [7].

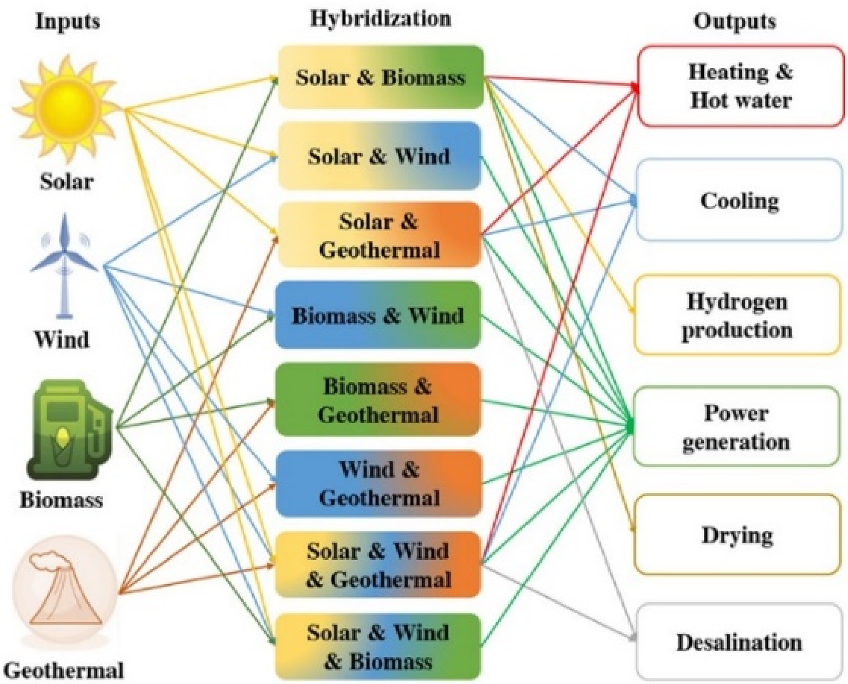

Fig. 2. Different systems of HRES [13].

Figure 2 illustrates the different types of HRES and the diverse usage of the output. Solar energy can be integrated into many HRESs. It is rich and environmentally friendly. The cost of PV panels has dropped significantly from 8 USD/W in 2008 to 1 USD/W today, which is an average annual decrease of 62% [25]. However, due to the disadvantage of instability, direct dependence on solar radiation, it is recommended to use solar energy in combining with other energy sources [16].

Amongst different types of renewable energy, biomass is the 4th largest source of energy [26]. Many researchers have studied combining the use of biomass with other RESs. Perkins [27] studied the cost of energy (COE) of solar-biomass HRES and concluded that the COE of this solution is cheaper than that of the plants using biomass or solar energy separately with battery storage devices. The electricity from biomass, especially from biogas, can be produced independently daytime or nighttime, under different weather conditions, thus it is possible to adjust the energy supply to meet the needs of the load [28]. The flexible operation of solar-biogas HRES helps to improve power quality and energy efficiency, leading to a reduction in COE, bringing benefits for the entire economy [28]. In addition, the increasing proportion of flexible biogas installations will reduce the need for traditional power plants, which are characterized by relatively high operating costs and pollutant emissions [28]. Therefore, biogas can be considered as a solution to stabilize the solar power system, which depends on random changes of solar radiation [28]-[30].

Integrated solar-biogas power generation systems are becoming a popular choice for remote areas or regions lacking power grid [31]. Around the world, large-scale biogas production projects are concentrated in Europe and in North America [32]. In developing countries, biogas is produced on a small scale in households, livestock farms, but with a very large number of digesters, especially in rural areas. On the other hand, the areas lacking access to electricity today are mostly in Africa and South Asia, where solar power is abundant. Therefore, the combination of solar and biogas is an attractive option for the electrification of these areas [31], [33].

The solar-biogas HRES can safely and efficiently provide energy to grid-connected and off-grid communities [34]. It consists of PV panels, a power converter, and a biogas fueled generator [21]. The system can operate stably and efficiently when connected to the grid or not. Many studies have been carried out to evaluate the economic-technical efficiency of the solar-biogas HRES. Nixon et al. [35] conducted a study on economic, environmental, and technical issues of the solar-biomass HRES. Conclusions drawn from the study show that hybrid systems are more cost-effective than single RES for power generation [35]. Rajbongshi et al. [36] performed the design and optimization of combined PV/biomass/diesel systems for different load configurations. The results of the study indicate that a grid-connected system is more economically viable than an off-grid system in the same load configuration. Ahmad et al. [37], Rajbongshi et al. [36] conducted studies on the technical and economic viability of grid-connected and off-grid combined systems. The authors concluded that for remote areas, an off-grid solution can be more cost-effective than a grid-connected solution. Shahzad et al. [38] analyzed the technical and economic efficiency of an off-grid solar-biogas HRES and found that the system is reliable and cost-effective. Solar-biogas HRES are more technically feasible in providing a stable source of energy to residential communities in remote areas [31]. This system is also more economically beneficial than other solutions [39].

Although renewable energy such as solar energy and biogas has shown great research interest in the energy field with very large publications, the HRES using these energy sources remains an area of further research with a limited number of publications [2]. In the past decades, the research works on HRES have mainly focused on economic-technical features, sizing calculations and solutions for optimal coordination of energy sources in the system [40]. It is important and urgent now to shape the HRES modules with available components so that people in remote areas can install themselves the solar-biogas HRES, without special technical assistance.

Currently the basic components for installing solar-biogas HRES such as PV panels, inverter, and energy storage devices such as battery, hydrogen electrolyser can be found in the market. However, the internal combustion engine fueled with biogas-hydrogen integrated into the system have not been widely available. In practice, the characteristics of the engine depend on the fuel supply and operating conditions. In the solar-biogas HRES, the energy storage can be done through hydrogen instead of the battery. Therefore, the engine of the system can run on biogas-hydrogen blend with variable compositions. On the other hand, because the generator provides only additional energy to the system, the loading regime of the engine changes frequently. These characteristics of the engine need to be studied to improve the overall efficiency of the solar-biogas HRES. The availability of biogas-hydrogen engine will also promote a large application of solar-biogas HRES in remote areas.

This paper focuses on studying the solar-biogas HRES for energy supplying in a case study in rural area of Vietnam. Based on the analysis of energy consumption and solar power fluctuation in the region, the operating conditions of the biogas-hydrogen engine of the HRES were identified. The performance and emissions of the engine in such conditions were predicted by simulation.

2. MATERIAL AND METHODS

2.1 Survey of Power Consumption

Information on power consumption is required to design a suitable hybrid energy system. In this study, we carried out the survey of electricity consumption in Hoa Vang, a suburban district of Da Nang, Vietnam. This is a district with diverse activities of production such as agriculture, animal husbandry, silk weaving, aquaculture, and fishing. A small part of the district's population is involved in the production of handicrafts, business, and tourism services.

Household power consumption

Statistics on electricity consumption of 13,480 households in Hoa Vang district show that electricity demand has increased slightly over the years. Average monthly household electricity consumption Q increased from 161 kWh/month in 2018 to 170 kWh/month in 2019 and 179 kWh/month in 2020, equivalent to an average increase of about 4% per year (Figure 3a). In all surveyed years, power consumption is highest in summer. The maximum capacity of households is not so high, most of them are below 2kW (Figure 3b).

Business households' electric consumption

Figure 4a shows that the average electricity consumption of business households is stable over the years, at 630 kWh/month. Like households, electricity consumption of business households also increases during the summer months. The peak power consumption of most business households is less than 6 kW (Figure 4b). A few business households have peak power levels in the range of 8-10kW.

Livestock farm electric consumption

The electricity consumption of livestock farm is stable, at about 558 kWh/month over the years (Figure 5a). Electricity consumption in the summer is always at the highest level of the year. This is because livestock farms have to increase cooling capacity of the camps to ensure animal safety. Although the electric consumption is compatible with the business household, the peak power of the livestock farm is rather high. This is due to many operations of the farm must be carried out simultaneously at certain moments. The peak capacity of livestock households is lower than 10 kW (Figure 5b).

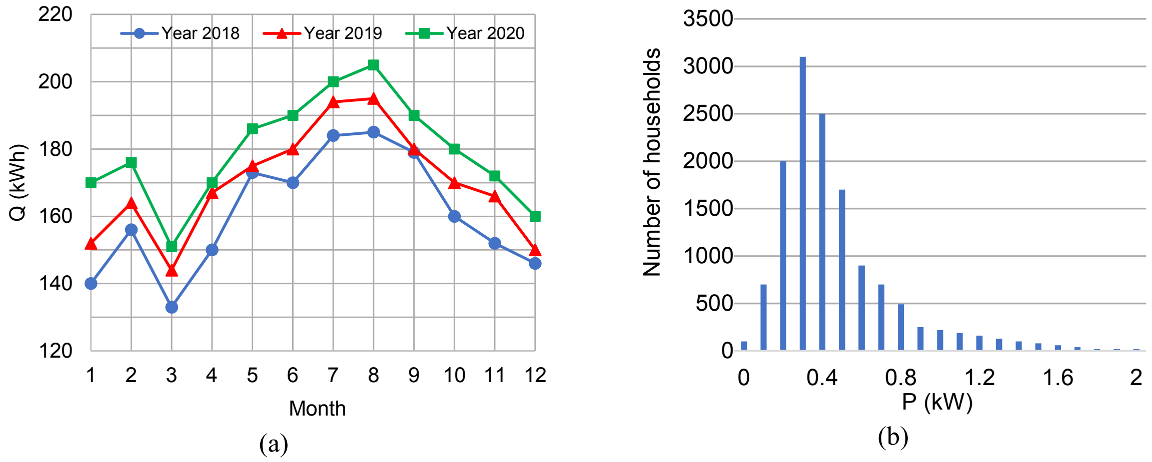

Fig. 3. Monthly electric consumption of household (a) and distribution of power in Hoa Vang (b).

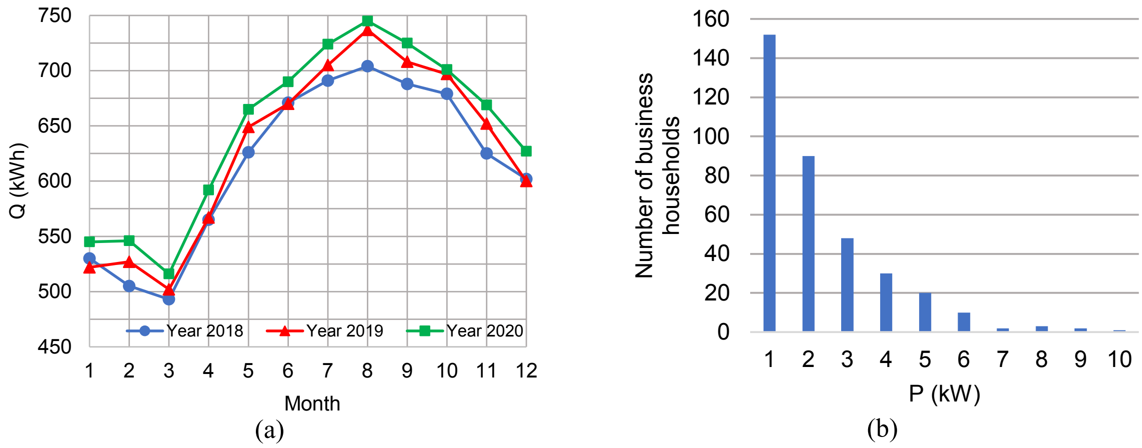

Fig. 4. Monthly electric consumption of a business household (a) and power distribution in Hoa Vang (b).

Figure 6 presents the daily variation of electricity power generated from a 5 kWp solar power plant in Danang area. From January to March, clear sky, light sunny, cloudy sometimes, the power fluctuated but the amplitude was not too large (Figure 6a). Maximum radiation is reached in the summer. The solar power plant starts generating electricity by 5:30 and ends by 17:00. Power varies with the radiation intensity and reaches its maximum at noon (Figure 6b). The rainy season start often in September in the region. It is cloudy, and solar radiation decrease (Figure 6c). At the last months of the year, it is heavy cloudy, the humidity in the air is very high, reducing solar radiation to the solar power station (Figure 6d).

This statistical result shows that the capacity compensation system for solar power stations must operate frequently during the day in the last months of the year. In the first months of the year, especially in summer, the power compensation system is needed mainly at night.

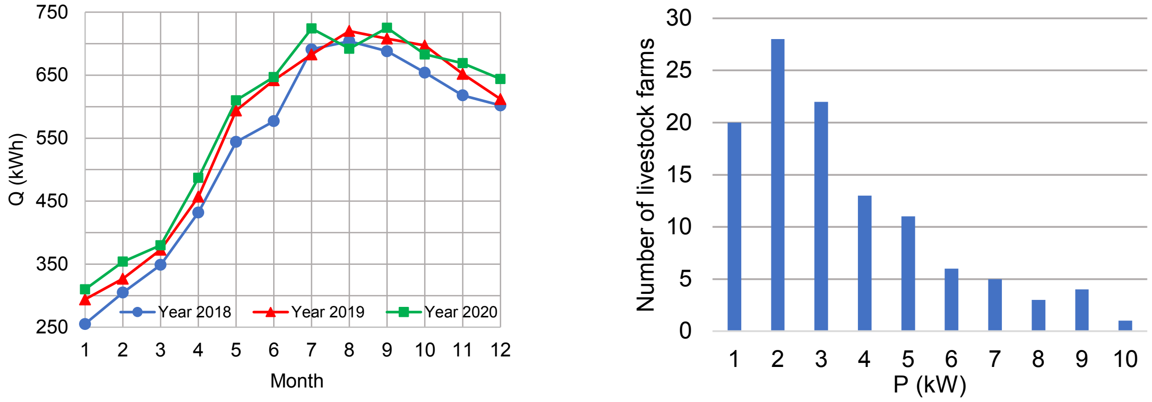

(a) (b)

Fig. 5. Monthly electric consumption of a livestock farm (a) and power distribution in Hoa Vang (b).

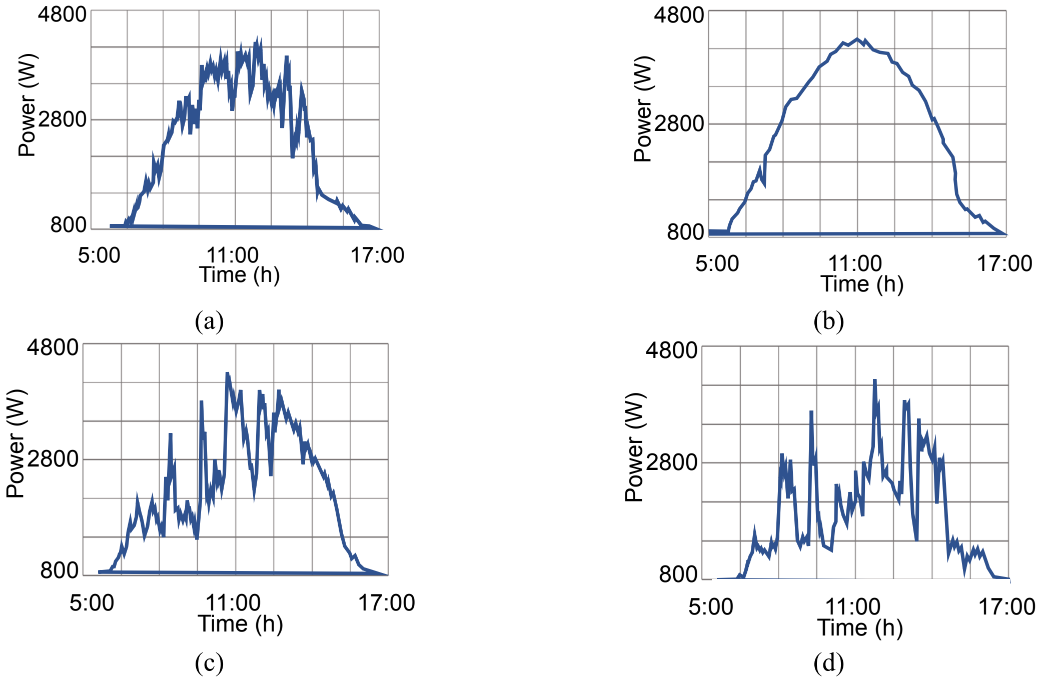

Fig. 6. Daily power variation in March (a), June (b), September (c) and December (d) in Danang region (Solar power plant 5 kWp).

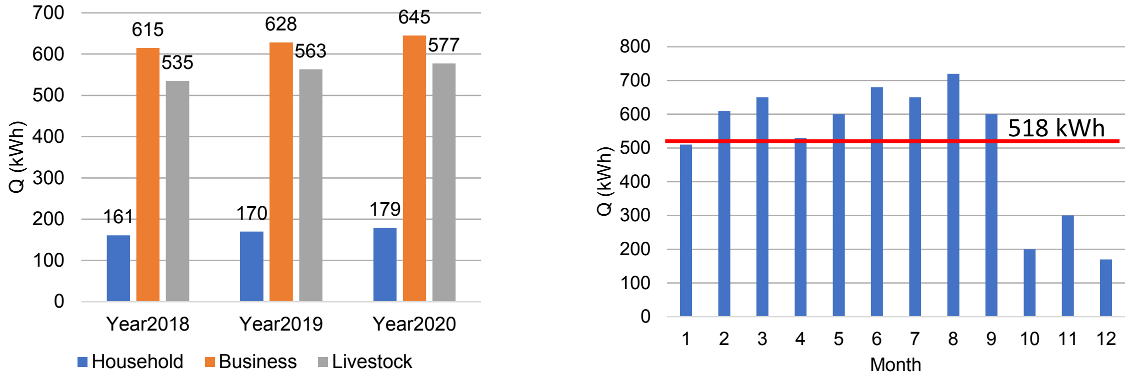

(a) (b)

Fig. 7. Average monthly electric consumption (a) and energy produced by a 5kWp solar plant (b).

Figure 7a summarizes the average monthly electricity consumption of households, business households and livestock farms in Hoa Vang. It can be seen that the electricity consumption of all local households and businesses does not exceed 650k Wh/month. According to the electricity system development plan in Vietnam, in the coming years, power consumption as well as peak capacity will increase by about 10%/year on average. Therefore, power systems must be designed with an excess capacity to ensure long-term operation of the system.

Figure 7b shows the electricity generated from a rooftop solar power plant with a capacity of 5kWp. As compared to the electric consumption in Figure 7a, the power of solar-biogas HRES can be chosen 3kWp, 6kWp and 7kWp, respectively for households, livestock farms and business households. In terms of energy balance, the solar power system with these capacity sizes alone can meet the requirements of the loads. However, as analyzed above, solar power capacity varies by hour of the day and by month of the year. Therefore, the power compensation system must ensure to provide enough energy when the solar power capacity decreases or stops supplying. In this study, biogas-hydrogen generator is used as the power compensation source. For households, to ensure stable power in the daytime as well as in the nighttime, generator capacity can be chosen 3 kW. For the business households, due to the main operation is in the daytime with the peak capacity is 6 kW, we can choose a generator capacity of 5 kW for energy compensation. In the case of the livestock farms, although the electric consumption level is low, they need a high peak power to ensure operation in the daytime as well as in the nighttime. With abundant biogas source of livestock farms, a generator of 10 kW is suitable for the HRES of this sector.

Basically, these systems only differ in the capacity of the PV panels and size of the generator. The control system, switching devices and displaying parameters is not quite different. The capacity of each PV panel is normally 370 Wp, so we need 9 panels for a 3kWp plant.

2.2 *Concept of Solar-Biogas HRES*

Figure 8 presents the schema of solar-biogas HRES. In this system, hydrogen is used for energy storage instead of battery. Hydrogen is produced from the electrolysis of water. When the PV panels power is higher than the required power of load, the excess energy is supplied to the water electrolyser to produce hydrogen. Hydrogen is then blended with biogas to fuel the generator. Conversely, when the load capacity is higher than the power generated from the PV panels, the microcontroller will disconnect the water electrolyser, open the solenoid valve of biogas-hydrogen storage tank, start the engine to generate an additional power.

The system is controlled by the energy management program integrated in the processor. The sensor node of the system supplied the parameters such as current, voltage, power consumption of the AC load, DC voltage of the PV panels, AC power of the generator and switch ON/OFF different contactors ensure the smooth operation of the system. The capacity of the PV panels and the power consumption of the load are measured in real time. The measured values from the sensor are periodically sent to the central node through the LoRa module to update the data storage system. The system was tested in off-grid mode.

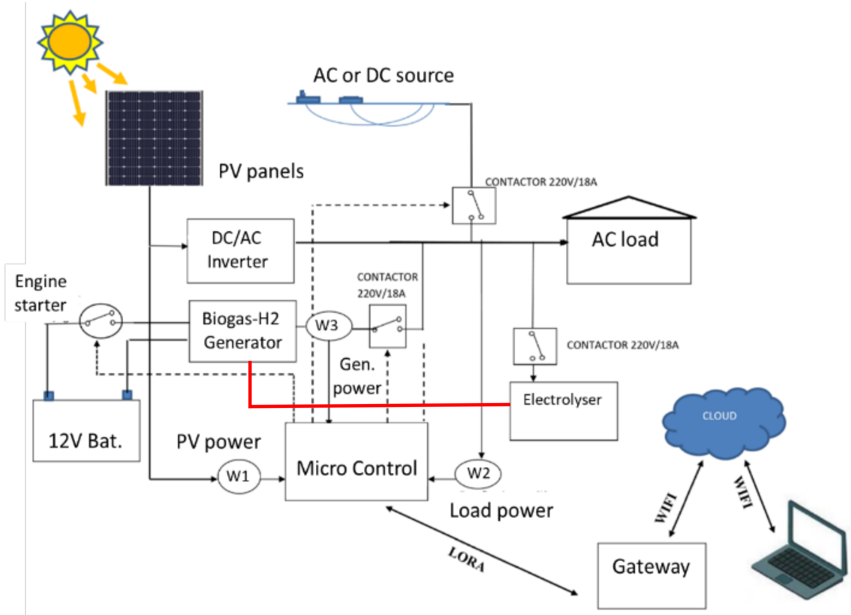

Fig. 8. Schema of biogas-solar HRES.

2.3 *Biogas-Hydrogen Engine in the HRES*

Biogas-hydrogen engine was converted from the SI stationary Honda GX200 engine. Technique of the conversion was presented in [41]-[43], [56]. Engine specifications are given in Table 1.

Table 1. Engine specifications.

Type of engine	1 cylinder, 4 strokes
Rated power (kW/rpm)	4.8/3600
Maximum torque (Nm/rpm)	12.4/2500
Displacement (cm^3)	196
Bore x stroke (mm)	68 x 54
Ignition timing	20° before TDC
Compression ratio	8.5 : 1

The original fueling system of the engine is replaced by an electronic control system including sensors, gas injectors and ECU. In this work, the set of sensors of the Honda motorcycle gasoline injection engine was used to adapt the conversion engine [44], [56]. Due to the injection map and ignition map have been changed, the ECU must be set up. In this work, we used the open ECU APITech for this purpose. The system configuration, maps installation and other supplement commands of the adaptation engine can be saved in the ECU memory. Figure 9 presents the schema of control system of the converted engine.

The sensors provide operating parameters including engine speed, loading regime, intake air flow, temperature, TDC position so that ECU calculates the injection duration and the advance ignition angle according to the engine maps saved in the memory. In addition, the oxygen sensor in the exhaust gas manifold sends a feedback signal about the excess air so that the ECU can adjust the biogas-hydrogen injection, accordingly, ensuring the equivalence ratio of the mixture is always in stoichiometric range.

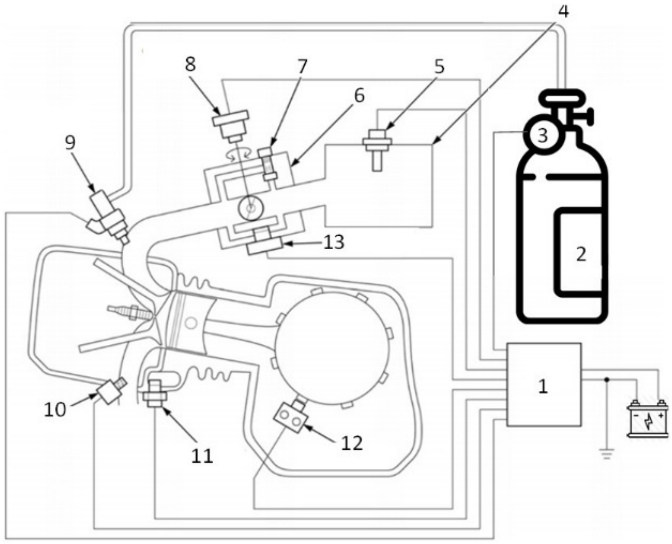

Fig. 9. Electronic control system for biogas-hydrogen engine converted from Honda GX200 stationary SI engine
1. ECU, 2. Biogas-hydrogen cylinder, 3. Solenoid valve, 4. Air filter, 5. IAT (Intake Air Temperature) sensor, 6. Throttle body, 7. Idlling air control, 8. TP (Throttle Position) sensor, 9. Biogas-hydrogen injector, 10. Oxygen sensor, 11. Engine temperature sensor, 12. CKP (Crankshaft Position) sensor, 13. Idle speed control valve

2.4 Method

Characteristics of biogas-hydrogen engine were studied by simulation. The commercial ANSYS FLUENT 18.2 CFD code was used for the purpose. The meshing of the calculation space was generated automatically by meshing procedure included in the workbench. The mesh distorsion in the cylinder due to the piston displacement was described via dynamic mesh. To reduce the calculation time, the intake manifold was deactivated at closure of the intake valve.

In the simulation, the k-ε turbulence model was used to close the convection-diffusion equations system. The partially premixed combustion model was used to describe the combustion process of biogas-hydrogen with air. The combustion products were considered in thermodynamic equilibrium, except NO_x concentration which was determined via the thermal mechanism of Zeldovich.

The pressure and temperature of air at the inlet port; the presure, temperture and fuel compositions at the nozzle of the injector were introduced at each calculation. The thermodynamic properties and the equivalence ratio of the gas mixture were determined via the concentrations of CH_4, H_2 and air in the cylinder in compression stroke. The details of simulation set up were presented in [44]-[45].

3. RESULTS AND DISCUSSION

The effect of hydrogen-enriched biogas in full load mode of the engine has been published by many authors [46]. Ilbas et al. [47] found that when the hydrogen content increased, the burning rate increased, and the flame limit is widened. Porpatham et al [48] studied the effect of equivalence ratio on the performance of the engine fueled with biogas enriched by 5%, 10% and 15% in volume of hydrogen. The results show that the burning rate increases with the hydrogen content in the fuel mixture. Simulation study by Bui et al. [44] shows that when increasing the hydrogen content in biogas mixture, the optimal advance ignition angle decreases. Enrichment biogas by hydrogen can improve the engine performance, reduce CO and HC emissions, but lead to an increase in NO_x emission [49]. This is due to the close relationship between NO_x emissions and maximum combustion temperature [44]-[46], [49]. Wang et al. [51] found that the heat release rate and NO_x emissions increased with the hydrogen content in fuel mixture, and they suggested that a 20% blend of hydrogen by volume in mixture containing of methane is optimal for achieving a balance between engine efficiency and pollution emissions. In most cases, hydrogen can be considered as an effective additive for biogas to improve fuel properties. Using biogas-hydrogen blend on internal combustion engine of solar-biogas HRES is thus, a promising solution for energy saving and GHG emission reduction [52]-[55].

Most of the research results on biogas-hydrogen engines found in the literature revealing the engine characteristics in full load operating condition. In the HRES, as it has been mentioned above, biogas-hydrogen generators only provide compensating capacity for the solar power system. Therefore, in the daytime, the engine mainly operates in partial loading mode, but in the nighttime, it operates mainly at full loading mode. Generally, the loading mode of the engine changes more often. This is the main difference of the engine in the HRES as compared to the stationary engines.

Figure 10a shows effects of loading regime on combustion characteristics of the engine fueled with biogas M7C3 at 3600 rpm with equivalence ratio $\phi = 1$, advance ignition angle $\varphi_S = 32°CA$. The indicative engine cycle work is 172.82, 165.04, 138.28 and 103.72 J/cyc corresponding to 100%, 75%, 65% and 50% engine load, respectively. At low loading regime, the combustion takes place not completely, so CO and HC emissions increase. Figure 10a shows that at 50% loading mode, CO and HC emissions are doubled compared to full loading mode. Due to the low engine loading mode, the combustion continues to take place in the expansion process, therefore the maximum temperature decreases leading to a reduction in NO_x emission. The result shows that the NO_x concentration in the exhaust gas at 50% engine loading mode is reduced by 50% compared to the full loading mode.

Figure 10b shows effects of loading mode on the combustion characteristics of the engine fueled with M7C3-20H2 at 3600 rpm with equivalence ratio $\phi = 1$, advance ignition angle $\varphi_S = 32°CA$. The indicated engine cycle work is 195.64, 133.95 and 104.23 J/cyc, corresponding to 100%, 65% and 50% load regime, respectively. At the 50% loading mode, the CO and HC emissions are doubled compared to the full loading mode, but the NO_x concentration is reduced by 60% (Figure 10b).

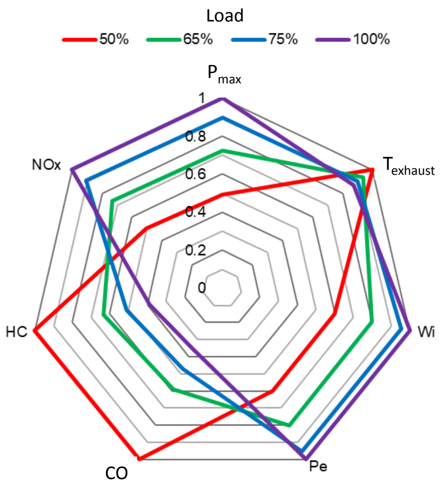

(a)

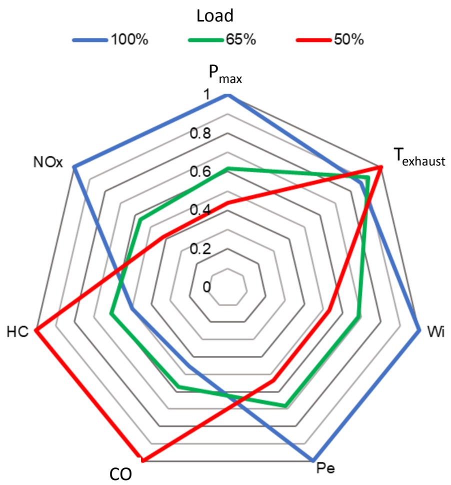

	Scale	
Fuel	M7C3	M7C3-20H2
P_{max} (bar)	26.56	30.2
$T_{exhaust}$ (K)	1871	1803
Wi (J/cyc)	172.82	195.64
Pe (kW)	3.89	4.4
CO (%V)	0.17	0.12
HC (%V)	0.06	0.05
NO_x (ppmV)	816	1053

(b)

Fig. 10. Effects of engine loading regimes on combustion characteristics of the engine fueled with biogas M7C3 (a) and with M7C3-20H2 (b) (n = 3600 rpm, $\phi = 1$, $\varphi_s = 32°CA$).

The above results show that the indicative engine cycle work increases with the increase of hydrogen content in the mixture with biogas. Figures 10a and 10b show that as adding 20% hydrogen into biogas M7C3, the indicative engine cycle work increases by 13% at full loading mode. With the same addition of hydrogen, the indicative engine cycle work increases by 4% and 2% at 65% loading mode and 50% loading mode, respectively as shifting from biogas M7C3 to blend fuel M7C3-20H2. Effect of hydrogen on improvement of indicative engine cycle work is reduced at partial loading mode operation. Like the full loading mode, in partial loading mode, the addition of hydrogen to biogas results in a decrease in CO and HC emissions, but an increase in NO_x emissions.

Figure 11a shows the effect of advance ignition angle on in-cylinder pressure variation when the engine is fueled with M7C3-20H2, operating at 3600 rpm, 60% load. When the engine load decreases, both temperature and pressure of the mixture in the cylinder decrease. The relationship between the laminar flame speed S_L with pressure and temperature can be expressed as $S_L = S_{Lo}T^a/P^b$, where a, b are positive coefficients, S_{Lo} is laminar flame speed at normal condition. When the engine load decreases, the pressure decreases, so S_L increases, but the temperature also decreases, so S_L decreases. Combining the effects of pressure and temperature, the laminar flame speed at partial loading mode is practically equivalent to that at full loading mode.

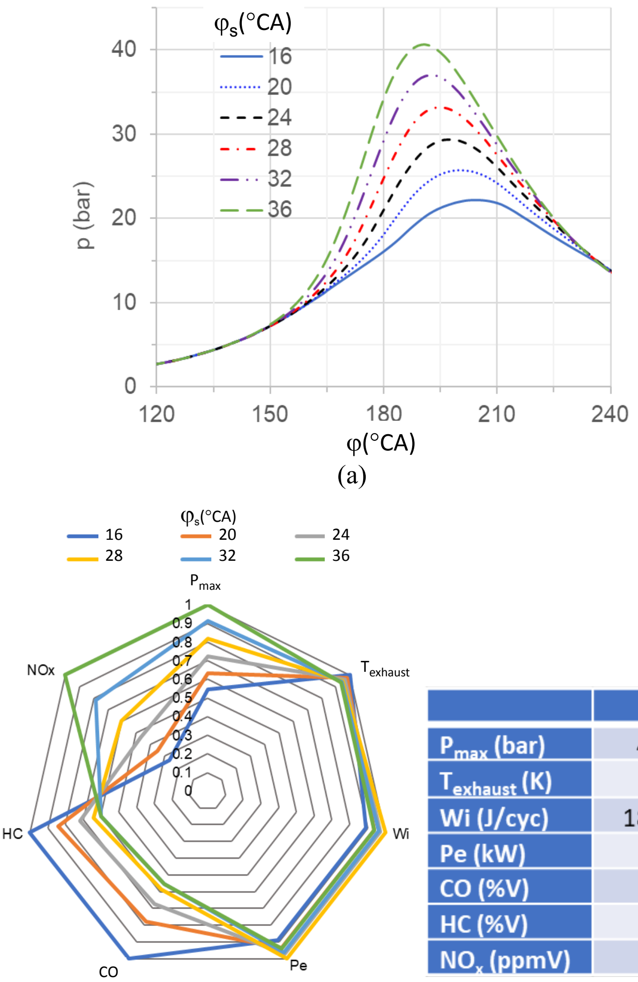

	Scale
P_{max} (bar)	40.62
$T_{exhaust}$ (K)	1600
Wi (J/cyc)	183.04
Pe (kW)	4.12
CO (%V)	0.06
HC (%V)	0.03
NO_x (ppmV)	2679

Fig. 11. Effects of advance ignition angle on in-cylinder pressure (a), and on combustion characteristics (b) of engine fueled with M7C3-20H2 (n = 3600 rpm, ϕ = 1).

Figure 11b shows the influence of advance ignition angle on combustion characteristics of the engine running at 60% load, 3600 rpm fueled with M7C3-20H2, and ϕ = 1. It can be observed that the increase of advance ignition angle results in an increase in NO_x concentration but a decrease in CO, HC emissions. This is due to the reduction of reaction rates with the decrease of pressure and temperature resulted from partial load operating mode. The variation of Wi according to the advance ignition angle in the case of partial load operating mode is similar to that of full loading mode. The optimal advance ignition angle in this case of 60% load is 28°CA, equivalent to that of full loading regime when the engine is fueled with the same fuel.

The research results show that at a given speed and engine loading mode, the optimal equivalence ratio and the optimal advance ignition angle decrease when CH_4 composition in biogas or/and H_2 content in fuel mixture increase as shown in Table 2. It can be seen that the advance ignition angle decreases by 4°CA when the CH_4 concentration in biogas increases from 60% to 80% or when adding 20% hydrogen to biogas.

Table 2. Effects of CH_4 concentration and H_2 content on the optimal equivalence ratio and the optimal advance ignition angle.

Biogas	M6C4		M7C3		M8C2	
H_2 content	0%	20%	0%	20%	0%	2%
ϕ	1.05	1.005	1.03	1.003	1.01	1.002
φ_s	32	28	30	26	28	24

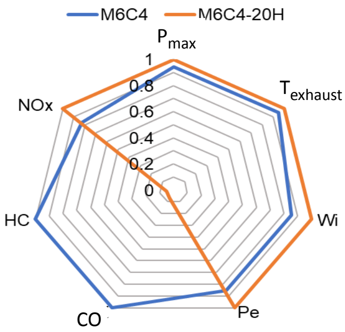

(a)

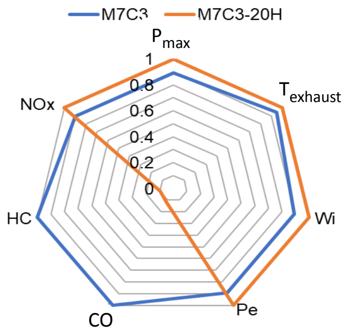

(b)

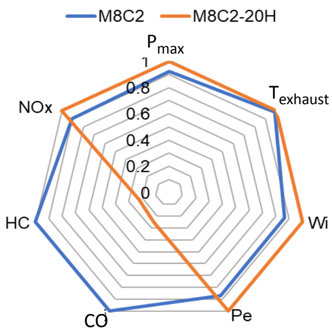

	Scale		
Fuel	M6C4, M6C4/0-20H2	M7C3, M7C3/0-20H2	M8C2, M8C2/0-0/20H2
P_{max} (bar)	34	37	38
$T_{exhaust}$ (K)	1535	1584	1547
Wi (J/cyc)	188	190	202
Pe (kW)	4.23	4.27	4.54
CO (%V)	0.55	0.34	0.16
HC (%V)	0.35	0.22	0.11
NO_x (ppmV)	1216	1804	2101

(c)

Fig. 12. Comparison of combustion characteristics of the engine fueled with neat biogas M6C4 (a), M7C3 (b), M8C2 (c), and with biogas enriched by 20% hydrogen under optimal operating conditions.

Figures 12a, 12b, and 12c compare the combustion characteristics and pollutant emissions of the engine fueled with neat biogas and with biogas enriched by 20% hydrogen operating under the optimal conditions given in Table 2. It can be observed that with any biogas, the presence of hydrogen in the fuel mixture also helps to improve combustion efficiency, consequently, enhance indicative engine cycle work. The indicative engine cycle work increases by 13% with the addition of 20% hydrogen to biogas. Besides, biogas enriched by 20% hydrogen can reduce the CO and HC emissions by 5 times with M8C2 and by 10 times with M6C4 in optimal operating conditions. The downside when adding hydrogen into biogas is the increase of NO_x emission. These results show that under optimal conditions, NO_x emissions increase about 10-15% when 20% hydrogen is added to biogas.

4. CONCLUSION

Solar-biogas HRES is promising solution for electrification of rural area in the developing countries. It is particularly suitable for remote regions where the extension of power network is not cost-effective. Solar-biogas HRES can operate in grid connected mode or off-grid mode. The cost of energy of HRES is lower than that of conventional power production plants [36]-[39]. Biogas-hydrogen engine is an important component of the solar-biogas HRES. Partial load operating mode of the engine affects the global performance of the system. The following conclusions can be drawn from the above research:

- Solar-biogas HRES with PV panels capacity of 3, 6 and 7 kWp and biogas-hydrogen engine capacity of 3, 10 and 5 kW is suitable for households, livestock farms and business households, respectively in case study of Danang region. The biogas-hydrogen engine operates mostly in the nighttime and during the last months of the year to supply the additional energy.
- Solar-biogas HRES can be built up with mostly available components in the market. The electronic controlled biogas-hydrogen engine of the HRES can

be converted from a conventional gasoline engine by adapting the injection system of a fuel injection gasoline motorcycle.

- Hydrogen is an effective solution for energy storage of the solar-biogas HRES. Hydrogen generated from the system can be used as an additive to biogas to improve combustion characteristics of the engine. Addition of 20% hydrogen into biogas M7C3 leads to an increase in indicative engine cycle work by 13%, 4% and 2% at 100%, 65% and 50% loading mode, respectively.
- Independently loading regime, the addition of hydrogen to biogas results in a decrease in CO and HC emissions, but an increase in NO_x emissions. As compared to full loading mode, CO and HC emissions of the engine are doubled, but the NO_x concentration in the exhaust gas drop down 50% in the half load operating mode.
- At a given speed and engine loading mode, the optimal equivalence ratio and the optimal advance ignition angle decrease when CH_4 composition in biogas or/and H_2 content in fuel mixture increases. The optimal advance ignition angle decreases by 4°CA as CH_4 concentration increases from 60% to 80% or as adding 20% hydrogen to biogas.

With the optimal equivalence ratio and advance ignition angle, as compared to neat biogas, the enrichment 20% hydrogen to biogas can reduce the CO and HC emissions by 5 times with M8C2 and by 10 times with M6C4, but an increase in NO_x emission about 10-15% in average.

ACKNOWLEDGEMENT

The authors wish to express their appreciation to the Ministry of Education and Training for supporting this research under project number B2021-DNA-03 "Power generation via RDF produced from solid waste in rural area”.

NOMENCLATURE AND ABBREVIATION

°CA	Degree of crankshaft angle
CFD	Computational Fluid Dynamics
ECU	Electronic Control Unit
GHG	Greenhouse gas
HRES	Hybrid Renewable Energy System
MxCy	Biogas compositions, where 10x is the composition of methane and 10y is the composition of CO_2 (in % volume)
MxCy-zH2	Blend of biogas MxCy and z% hydrogen
n	Engine speed (rpm)
P_e	Brake power (kW)
P_{max}	Maximum in-cylinder pressure (Bar)
PV	Photovoltaic
RES	Renewable energy sources
SI	Spark ignition
T	Temperature of the gas mixture in cylinder (K)
TDC	Top Dead Center
$T_{exhaust}$	Temperature of exhaust gas (K)
Wi	Indicative engine cycle work (J/cyc)
φ	Crankshaft angle (°CA)
ϕ	Equivalence ratio
φ_s	Advance ignition angle (°CA before TDC)

REFERENCES

[1] IEA, 2021. Global population without access to electricity by region, 2000-2021. https://www.iea.org/data-and-statistics/charts/global-population-without-access-to-electricity-by-region-2000-2021-2.

[2] The World Bank, 2021. Report: Universal Access to Sustainable Energy Will Remain Elusive Without Addressing Inequalities. https://www.worldbank.org/en/news/press-release/2021/06/07/report-universal-access-to-sustainable-energy-will-remain-elusive-without-addressing-inequalities.

[3] Robert F.C. and S. Gopalan. 2018. Low cost, highly reliable rural electrification through a combination of grid extension and local renewable energy generation. *Sustainable Cities Society* 42: 344-354. https://doi.org/10.1016/j.scs.2018.02.010.

[4] Khodayar M.E., 2017. Rural electrification and expansion planning of off-grid microgrids. *The Electricity Journal* 30: 68–74. https://doi.org/10.1016/j.tej.2017.04.004.

[5] Sigarchian S.G, Paleta R., Malmquist A., Pina A., 2015. Feasibility study of using a biogas engine as backup in a decentralized hybrid (PV/wind/battery) power generation system - case study Kenya. *Energy* 90: 1830-41. https://doi.org/10.1016/j.energy.2015.07.008.

[6] Yousefi H., Ghodusinejad M.H., Kasaeian A., 2017, Multi-objective optimal component sizing of a hybrid ICE + PV/T driven CCHP microgrid. *Applied Thermal Engineering.* https://doi.org/10.1016/j.applthermaleng.2017.05.017.

[7] Lian J., Zhang Y., Ma C., Yanga Y., and Chaima E., 2019. A review on recent sizing methodologies of hybrid renewable energy systems. *Energy Conversion and Management* 199: 1-23. https://doi.org/10.1016/j.enconman.2019.112027.

[8] Dujardin J., Kahl A., Kruyt B., Bartlett S., and Lehning M., 2017. Interplay between photovoltaic, wind energy and storage hydropower in a fully renewable Switzerland. *Energy* 135: 513-525. https://doi.org/10.1016/j.energy.2017.06.092.

[9] Silva A.R., Pimenta F.M., Assireu A.T., and Spyrides M.H.C., 2016. Complementarity of Brazil' s hydro and offshore wind power. *Renewable and Sustainable Energy Reviews* 56: 413-427. https://doi.org/10.1016/j.rser.2015.11.045..

[10] Zhou S., Wang Y., Zhou Y., Clarke L.E., and Edmonds J.A., 2018. Roles of wind and solar energy in China’s power sector: implications of intermittency constraints. *Applied Energy* 213:22-

30. https://doi.org/10.1016/j.apenergy.2018.01.025.

[11] Ataei A., Nedaei M., Rashidi R., and Yoo C., 2015. Optimum design of an off-grid hybrid renewable energy system for an office building. *Renewable Sustainable Energy* 7(5): 1-25. https://doi.org/10.1063/1.4934659.

[12] Khatib T., Mohamed A., Sopian K., and Mahmoud M., 2015. Optimal sizing of hybrid pv/wind systems for Malaysia using loss of load probability. *Energy Sources Part A: Recovery, Utilization, and Environmental Effects* 37(7): 687-695. https://doi.org/10.1080/15567036.2011.592920.

[13] Guo S., Liu Q., Sun J., and Jin H., 2018. A review on the utilization of hybrid renewable energy. *Renewable and Sustainable Energy Reviews* 91 1121–1147. https://doi.org/10.1016/j.rser.2018.04.105.

[14] Chouaib A., Djamel B., Batoul T., and Salim M., 2021. Sizing, optimization, control and energy management of hybrid renewable energy system- a review. *Energy and Built Environment*, In Press, Available online 4 May 2021, doi: https://doi.org/10.1016/j.enbenv.2021.04.002.

[15] Come Zebra E.I., Henny J.W., Nhumaio G., and Faaij A.P.C., 2021. A review of hybrid renewable energy systems in mini-grids for off-grid electrification in developing countries. *Renewable and Sustainable Energy Reviews* 144. In Press, Available online July 2021, https://doi.org/10.1016/j.rser.2021.111036.

[16] Jaszczur M., Hassan Q., Palej P., and Abdulateef J., 2020. Multi-Objective optimisation of a micro-grid hybrid power system for household application. *Energy* 202: 1-24. https://doi.org/10.1016/j.energy.2020.117738.

[17] Prebeg P., Gasparovic G., Krajacic G., Krajacic G., and Duic N., 2016. Long-term energy planning of Croatian power system using multi-objective optimization with focus on renewable energy and integration of electric vehicles. *Applied Energy* 184: 1493-507. https://doi.org/10.1016/j.apenergy.2016.03.086.

[18] Bär K., Saidi A., Hackl C., and Zörner W., 2019. Combined operation of photovoltaic and biogas plants for optimal transformer loading. *Chemical Engineering Transactions* 76: 601-606. DOI:10.3303/CET1976101.

[19] Pourbehzadi M., Niknam T., Aghaei J., and Mokryani G., 2019. Electrical Power and Energy Systems Optimal operation of hybrid AC/DC microgrids under uncertainty of renewable energy resources: a comprehensive review. *Electrical Power Energy Systems* 109: 139–59. https://doi.org/10.1016/j.ijepes.2019.01.025.

[20] Fathima A.H. and K. Palanisamy. 2015. Optimization in microgrids with hybrid energy systemse: A review. *Renewable Sustainable Energy Reviews* 45: 431-46.

[21] Ifegwu E., Anjaneyulu K., 2014. Sustainable rural development: solar/biomass hybrid renewable energy system. *Energy Procedia* 57: 1492-1501. doi: 10.1016/j.egypro.2014.10.141.

[22] Ismail M.S., Moghavvemi M., Mahlia T.M.I., Muttaqi K.M., and Moghavvemi S., 2015. Effective utilization of excess energy in standalone hybrid renewable energy systems for improving comfort ability and reducing cost of energy: a review and analysis. *Renewable Sustainable Energy Reviews*. 42: 726-34. https://doi.org/10.1016/j.rser.2014.10.051.

[23] Williams N.J., Jaramillo P., Taneja J., and Ustun T.S., 2015. Enabling private sector investment in microgrid-based rural electrification in developing countries: a review. *Renewable Sustainable Energy Reviews* 52: 1268-81. https://doi.org/10.1016/j.rser.2015.07.153.

[24] Soumya M., Hosna Y., Sarker M.R.I., and Beg M.R.A., 2017. Prospect of solar-PV/biogas/diesel generator hybrid energy system of an off-grid area in Bangladesh. Dhaka, Bangladesh, 22-23 Feb. 2017. *AIP Conference Proceedings 1919*, Published Online 28 December 2017; 020020_1-8 https://doi.org/10.1063/1.5018538.

[25] SUNRUN,2021. Cost of solar in 2021, https://www.sunrun.com/solar-lease/cost-of-solar.

[26] Borges Neto M.R., Carvalho P.C.M., Carioca J.O.B., and Canafistula F.J.F., 2010. Biogas/photovoltaic hybrid power system for decentralized energy supply of rural areas. *Energy Policy* 38: 4497-450. https://doi:10.1016/j.enpol.2010.04.004.

[27] Perkins G., 2018. Techno-economic comparison of the levelised cost of electricity generation from solar PV and battery storage with solar PV and combustion of biocrude using fast pyrolysis of biomass. *Energy Conversion Management.* https://doi.org/10.1016/j.enconman.2018.06.090.

[28] Bär K., Wagender S., Solka F., Saidi A., and Zörner W., 2020. Flexibility potential of photovoltaic power plant and biogas plant hybrid systems in the distribution grid. *Chemical Engineering and Technology* pp. 1-12. https://doi.org/10.1002/ceat.202000025.

[29] Häring G., Sonnleitner M., Bär K., Brown N., and Zörner W., 2017. Demonstration of controllable electricity production via biogas plants. *Chemical Engineering Technol*ogy 40: 298-305.

[30] Dotzauer M., Pfeiffer D., Lauer M., Pohl M, Mauky E, Bar K, Sonnleitner M, Zorner W, Hudde J, and Schwarz B, 2018. How to measure flexibility-performance indicators for demand driven power generation from biogas plants. *Renewable Energy* 134: 135-146. https://doi.org/10.1016/j.renene.2018.10.021.

[31] Tamoor M., Suleman T., Muhammad S., Muhammad B.T., Shahid I., Tasmia N., 2020. Design of 3 kW integrated power generation system from solar and biogas. *Hydrogen Energy*, 45(23): 12711-12720. https://doi.org/10.1016/j.ijhydene.2020.02.207.

[32] Torres R.A., Marin D., Rodero M.R., Pascual C., Gonzalez-Sanchez A., Crespo I.G., Lebrero R.,

and Torre R.M., 2020. Biogas treatment for H_2S, CO_2, and other contaminants removal. Recent Developments, New Trends, Advances, and Opportunities, Chapter 8: 153-176. DOI: https://doi.org/10.1016/B978-0-12-819064-7.00008-X.

[33] Kumar V. and N. Kaistha. 2020. Control of a concentrated solar power-biogas hybrid unit. IFAC Papers OnLine 53(1): 332-337.

[34] Agyenim F.B., Dzamboe P.D., Mohammed M., Dzamboe P.D., and Bawakyillenuo S., 2020. Powering communities using hybrid solar-biogas in Ghana, a feasibility study. *Environmental Technology & Innovation* 19(1), 100837. In Press, Available online April 2020. https://doi.org/10.1016/j.eti.2020.100837.

[35] Nixon J.D., Dey P.K., and Davies P.A., 2012. The feasibility of hybrid solar-biomass power plants in India. *Energy* 46: 541-54.

[36] Rajbongshi R, Borgohain D, and Mahapatra S., 2017. Optimization of PV-biomass-diesel and grid base hybrid energy systems for rural electrification by using HOMER. *Energy* 126: 461-74. https://doi.org/10.1016/j.energy.2017.03.056.

[37] Ahmad J, Imran M, Khalid A, Iqbal W, Ashraf SR, Adnan M., Ali S.F., and Khokhar K.S., 2018. Techno economic analysis of a wind-photovoltaic-biomass hybrid renewable energy system for rural electrification: a case study of Kallar Kahar. *Energy* 148: 208–34. https://doi.org/10.1016/j.energy.2018.01.133.

[38] Shahzad MK, Zahid A, Rashid T, Abdullah M., Muzaffar R., and Ahmad A.M., 2017. Techno-economic feasibility analysis of a solar-biomass off grid system for the electrification of remote rural areas in Pakistan using HOMER software. *Renewable Energy*: 106: 264-73. https://doi.org/10.1016/j.renene.2017.01.033.

[39] Ganthia B.P., Sasmita S., Rout K., Pradhan A., and Nayak J., 2018. An economic rural electrification study using combined hybrid solar and biomass-biogas system. *Materials Today: Proceedings* 5, 220-225.

[40] Krishna K.S. and K. Kumar. 2015. A review on hybrid renewable energy systems. *Renewable Sustainable Energy Reviews* 52: 907-916.

[41] Bui V.G, Tran V.N, and Truong L.B.T, 2013. Determination of Optimal Operational Parameters of SI Biogas Engines Converted from Diesel Engines by Modelling and Experimental Studies. In the Proceedings of *The 14th Asian Congress of Fluid Mechanics-14ACFM*, October 15-19,2013, Hanoi and Halong, Vietnam, pp. 819-824.

[42] Bui V.G. and V.N. Tran. 2014. Mixer design for high performance SI engine converted from a diesel engine. *International Journal of Engineering Research and Technology* 3(1): 2743-2760.

[43] Bui V.G. and V.N. Tran. 2014. Appropriate structural parameters of biogas SI engine converted from diesel engine. *IET Renewable Power Generation* 8:1-7.

[44] Bui V.G., Tran V.N., Hoang A.T., Bui T.M.T., and Vo A.V., 2020. A simulation study on a port-injection SI engine fueled with hydroxy-enriched biogas. *Energy Sources, Part A: Recovery, Utilization, and Environmental Effects,* In Press, Available online 10 August 2020, https://doi.org/10.1080/15567036.2020.1804487.

[45] Bui V.G., Bui T.M.T., Nguyen V.D., and Bui V.H., 2020. Analysis of combustion and NO_x formation in a SI engine fueled with HHO enriched biogas. *Environmental Engineering and Management Journal* 19(5): 317-327.

[46] Bui V.G., Tran V.N., Bui T.M.T, and Nguyen Q.T., 2018. Numerical simulation studies on performance, soot and NO_x emissions of dual-fuel engine fueled with hydrogen enriched biogas mixtures. *Renewable Power Generation* pp. 1-8 https://doi:10.1049/iet-rpg.2017.0559.

[47] Ilbas M., Crayford A.P., Yilmaz I., Bowen P.J., and Syred N., 2006. Laminar-burning velocities of hydrogen-air and hydrogen-methane-air mixture: an experimental study. *International Journal of Hydrogen Energy* 31: 1768-1779.

[48] Porpatham E., Ramesh A., and Nagalingam B., 2007. E ffect of performance of a biogas fueled spark ignition engine. *International Journal of Hydrogen Energy,* 32: 2057-2065.

[49] Demuynck J., Raes N., Zuliani M., De Paepe M., Sierens R., and Verhelst S., 2009. Local heat flux measurement in a hydrogen and methane spark ignition engine with a thermopile sensor. *International Journal of Hydrogen Energy* 34: 9857-9868.

[50] Mohammed Y.S., Mustafa M.W., and Bashir N., 2014. Hybrid renewable energy systems for off-grid electric power: Review of substantial issues. *Renewable and Sustainable Energy Reviews* 35: 527-539. http://dx.doi.org/10.1016/j.rser.2014.04.022.

[51] Wang J, Huang Z, Fang Y, Liu B, Zeng K, Miao H, and Jiang D., 2007. Combustion behaviors of a direct injection engine operating on various fractions of natural gas-hydrogen blends. *International Journal of Hydrogen Energy* 32(15): 3555-3564.

[52] Boretti A., 2010. Comparison of fuel economies of high efficiency diesel and hydrogen engines powering a compact car with a flywheel based kinetic energy recovery systems. *International Journal of Hydrogen Energy* 35: 8417-8424.

[53] Bui V.G., Nguyen V.H., Bui T.M.T., and Bui V.H., 2015: Utilization of poor biogas as fuel for hybrid biogas-diesel dual fuel stationary engine. *International Journal of Renewable Energy Research* 5(4): 1007-1015.

[54] Bui V.G., Tran V.N., and Truong L.B.T., 2008. Engines fueled by biogas: A contribution to energy saving and climate change mitigation. The 6th Seminar on Environment Science and Technology Issues Related to Climate Change Mitigation.

Japan-Vietnam Core University Program, Osaka, Japan, 26-28 November 2008.

[55] Bui V.G., Tran V.N., and Nguyen T.T.X, 2010. Utilization of biogas engines in rural area: A contribution to climate change mitigation. *Colloque International RUNSUD* 2010, pp. 19-31, Universite Nice-Sophia Antipolis, France, 23-25 Mars 2010.

[56] Pham Q.T. and T.M.T Bui. 2020. adaptation of a hydrogen-enriched biogas engine in a solar-biogas hybrid energy system. *International Journal of Engineering Research & Technology* 9(5): 812-819.